International Journal of Mechanical and Industrial Technology ISSN 2348-7593 (Online)
Vol. 5, Issue 1, pp: (36-52), Month: April - September 2017, Available at: www.researchpublish.com

Steady State Performance Analysis of Finite Oil Journal Bearings considering Fluid Inertia and Surface Roughness effect

[1]A. K. Bandyopadhyay, [2]S. K. Mazumder, [3]M. C. Majumdar

[1]Assistant Professor, Department of Mechanical Engineering, DR. B. C Roy Engineering College, Durgapur, West Bengal, India
[2]Professor, Department of Mechanical Engineering, DR. B. C Roy Engineering College, Durgapur, West Bengal, India
[3]Professor, Department of Mechanical Engineering, NIT, Durgapur, West Bengal, India

Abstract: **The effect of fluid inertia is generally neglected in view of its negligible contribution compared to viscous force in the analysis of hydrodynamic journal bearings. The fluid inertia effect cannot be neglected when the viscous force are of the same order of magnitude and then the fluid inertia effect is to be taken in the analysis when the Modified Reynolds number is around one. Since no machining surfaces are perfectly smooth so the assumptions of smooth surfaces can no longer be employed to accurately predict the performance characteristics of journal bearing systems. This theoretical work analyses the combined influence of surface roughness and fluid-inertia effects on performance characteristics of hydrodynamic journal bearing. The average Reynolds equation that modified to include the fluid inertia and surface roughness effect and is used with appropriate boundary conditions to obtain pressure profile in the fluid-film region. The solutions of modified average Reynolds equations are obtained using finite difference method and appropriate iterative schemes. The effects of surface roughness parameter, roughness orientation, and roughness characteristics of opposing surfaces including fluid-inertia effects simultaneously on circumferential fluid-film pressure distribution, load carrying capacity of the bearing are studied. The steady state bearing performance analysis is done through parametric study of the various variables like modified Reynolds number, eccentricity ratio, slenderness ratio, attitude angle, surface roughness parameter, surface pattern parameter. The variation of bearing load carrying capacity, attitude angle, end flow, friction parameters has been studied and plotted against various parameters.**

Keywords: **Modified Reynolds number, slenderness ratio, attitude angle, sommerfeld number, eccentricity ratio, journal bearings, fluid inertia, roughness pattern and roughness parameter**.

I. INTRODUCTION

In the classical hydrodynamic theory the basic assumptions include negligible fluid inertia forces in comparison to the viscous forces. Due to high velocity it is possible to arrive at such a situation where flow is laminar but the fluid inertia effect cannot be neglected and the classical Reynolds equation is not valid in such case. Pinkus and Sterlincht [4], have shown that the fluid inertia effect cannot be neglected when the viscous and the inertia forces are of the same order of magnitude. In recent times synthetic lubricants, low viscosity lubricants, are used in industries. Because of high velocity it is possible to attain such a situation where flow is laminar but fluid inertia forces are significant.

It has been pointed out that there is an intermediate regime in which the flow is still laminar but both viscous and inertia forces are significant. Consideration of fluid inertia effect may be one of the areas of recent extension of the classical lubrication theory. Among the few studies related to effect fluid inertia effect, Constatinescu and Galetuse [3] evaluated the momentum equations for laminar and turbulent flows in fluid film are evaluated by assuming that the shape of

velocity profiles is not strongly affected by the presence of inertia forces. Banerjee et. al [5] introduced an extended form of Reynolds equation to include the effect of fluid inertia, adopting an iteration scheme. Chen and Chen[14] obtained the steady-state characteristics of finite bearings including inertia effect using the formulation of Banerjee et al. [5]. Kakoty and Majumdar [7] used the method of averaged inertia in which inertia terms are integrated over the film thickness to account for the inertia effect in their studies. The above studies were mainly based on ideally smooth bearing surfaces.

The classical theory of hydrodynamic lubrication given by Reynolds does not consider the surface roughness of the elements having relative motion. When the fluid-film thickness in a journal bearing system is of the order of few micrometres, the surface roughness topography has a profound effect on bearing performance. In the design of high speed rotary machinery, consideration of surface roughness is importance to predict the steady state characteristics analysis of the hydrodynamic journal bearing. Hydrodynamic lubrication theory of rough surfaces has been developed by several researchers since more than a decade ago. A thorough review of theories of hydrodynamic lubrication of rough surfaces was presented by Elrod [8]. There are basically two approaches for calculating hydrodynamic pressure distribution and load capacity of partially lubricated surfaces. Flow simulation method of a randomly generated rough surfaces with known statistical properties over the surface area was used by Patir and Cheng[1-2]. Tonder[11] studied the lubrication of rough surfaces by Monte Carlo method. Majumdar and Hamrock [10] have determined the hydrodynamic load capacity of finite oil journal bearing adopting Patir and Cheng model, but expressed average gap height in an analytical form. In Majumdar and Hamrock [10] the asperity contact load was also estimated following Greenwood and Tripp [12] theory. Flow factor method was critically looked into by Tripp[13] theory.

In the present work, a modified average Reynolds equation and a solution algorithm are developed to include fluid inertia and surface roughness effects in the analysis of lubrication problems. The developed model is used to study the influence of fluid inertia and surface roughness effects on the steady state characteristics such as circumferential pressure, load carrying capacity, attitude angle and side leakage of a hydrodynamic oil journal bearing.

II. BASIC THEORY

A. Considering fluid Inertia Effect only:

The modified average Reynolds equation for fully lubricated surfaces is derived starting from the Navier-Stokes equations and the continuity equation with few assumptions. The non-dimensional form of the momentum equations and the continuity equation for a journal bearing may be written as (Figure. 1)

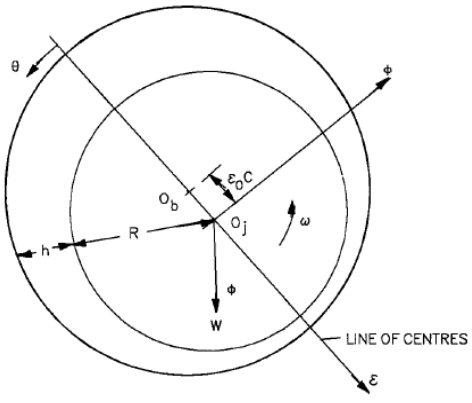

Fig. 1 The schematic diagram of flexibly supported oil Journal Bearing

$$R^*_e\left[\Omega\frac{\partial \bar{u}}{\partial \tau}+\bar{u}\frac{\partial \bar{u}}{\partial \theta}+\bar{v}\frac{\partial \bar{u}}{\partial \bar{y}}+\bar{w}\left(\frac{D}{L}\right)\frac{\partial \bar{u}}{\partial \bar{z}}\right]=-\frac{\partial \bar{p}}{\partial \theta}+\frac{\partial^2 \bar{u}}{\partial \bar{y}^2} \quad (1)$$

$$\frac{\partial \bar{p}}{\partial \bar{y}}=0 \quad (2)$$

$$R^*_e\left[\Omega\frac{\partial \bar{w}}{\partial \tau}+\bar{u}\frac{\partial \bar{w}}{\partial \theta}+\bar{v}\frac{\partial \bar{w}}{\partial \bar{y}}+\bar{w}\left(\frac{D}{L}\right)\frac{\partial \bar{w}}{\partial \bar{z}}\right]=-\left(\frac{D}{L}\right)\frac{\partial \bar{p}}{\partial \bar{z}}+\frac{\partial^2 \bar{w}}{\partial \bar{y}^2} \quad (3)$$

$$\frac{\partial \bar{u}}{\partial \theta}+\frac{\partial \bar{v}}{\partial \bar{y}}+\left(\frac{D}{L}\right)\frac{\partial \bar{w}}{\partial \bar{z}}=0 \tag{4}$$

Where, $\bar{z}=\frac{z}{L/2}$, $\bar{y}=\frac{y}{c}$, $\theta=\frac{x}{R}$, $\tau=\omega_p.t$, $\Omega=\frac{\omega_p}{\omega}$,

$\bar{u}=\frac{u}{\omega R}$, $\bar{v}=\frac{v}{c\,\omega}$ $\bar{w}=\frac{w}{\omega R}$ $\bar{p}=\frac{p c^2}{\eta \omega R^2}$ and

$R_e^*=R_e.\frac{c}{R}=\frac{\rho \omega c^2}{\eta}$

The variation in the density with time is considered to be negligible. Since there is no variation in pressure across fluid film the second momentum equation is not used.

The fluid film thickness can be given as

$$h=c+e\cos\theta \tag{5}$$

$$\bar{h}=1+\varepsilon\cos\theta \tag{6}$$

where, $\bar{h}=\frac{h}{c}, \varepsilon=\frac{e}{c}$,

After Constantinescu and Galetuse[3] the velocity components are approximated by the parabolic profiles. The velocity components may be expressed in non-dimensional form as follows:

$$\bar{u}=\left[\frac{\bar{y}}{\bar{h}}+Q_\theta\left(\frac{\bar{y}^2}{\bar{h}^2}-\frac{\bar{y}}{\bar{h}}\right)\right] \tag{7}$$

$$\bar{w}=\left[Q_z\left(\frac{\bar{y}^2}{\bar{h}^2}-\frac{\bar{y}}{\bar{h}}\right)\right] \tag{8}$$

Where, $\bar{u}=\frac{u}{\omega R}$, $\bar{w}=\frac{w}{\omega R}$, $\bar{y}=\frac{y}{c}$

Q_θ and Q_z are dimensionless flow parameter in θ and $\bar{z}$ direction respectively.

Substituting these two into momentum equations and integrating give

$$Q_\theta=\frac{\bar{h}^2}{2}\left(\frac{\partial \bar{p}}{\partial \theta}\right)+R_e^*\times I_X \tag{9}$$

$$Q_z=\frac{\bar{h}^2}{2}\left(\frac{D}{L}\right)\left(\frac{\partial \bar{p}}{\partial \bar{z}}\right)+R_e^*\times I_Z \tag{10}$$

Where,

$$I_X=\frac{\bar{h}}{2}\left[\begin{array}{l}\frac{1}{2}\Omega\left(1-\frac{1}{3}Q_\theta\right)\frac{\partial \bar{h}}{\partial \tau}-\frac{1}{6}\Omega\bar{h}\frac{\partial Q_\theta}{\partial \tau}-\frac{1}{3}\left(1-\frac{1}{2}Q_\theta+\frac{1}{10}Q_\theta^2\right)\frac{\partial \bar{h}}{\partial \theta}+\\ \frac{1}{3}\bar{h}\left(\frac{1}{5}Q_\theta-\frac{1}{2}\right)\frac{\partial Q_\theta}{\partial \theta}+\frac{1}{30}\left(\frac{D}{L}\right)\bar{h}\,Q_z\frac{\partial Q_\theta}{\partial \bar{z}}+\frac{1}{6}\left(\frac{D}{L}\right)\bar{h}\left(\frac{1}{5}Q_\theta-\frac{1}{2}\right)\frac{\partial Q_z}{\partial \bar{z}}\end{array}\right] \tag{11}$$

$$I_Z = \frac{\bar{h}}{2}\left[\begin{array}{l} -\frac{1}{6}\Omega\, Q_z \frac{\partial \bar{h}}{\partial \tau} - \frac{1}{6}\Omega \bar{h}\frac{\partial Q_z}{\partial \tau} - \frac{1}{6} Q_z \left(\frac{1}{5} Q_\theta - \frac{1}{2}\right)\frac{\partial \bar{h}}{\partial \theta} - \\ \frac{1}{6}\bar{h}\left(\frac{1}{5} Q_\theta - \frac{1}{2}\right)\frac{\partial Q_z}{\partial \theta} + \frac{1}{30}\bar{h} Q_z \frac{\partial Q_\theta}{\partial \theta} + \frac{1}{15}\left(\frac{D}{L}\right)\bar{h}\, Q_z \frac{\partial Q_z}{\partial \bar{z}} \end{array}\right] \quad (12)$$

Neglecting time depended terms one can obtain the following form of modified Reynolds equation for steady state condition considering fluid inertia effect.

$$\frac{\partial}{\partial \theta}\left(\bar{h}_0^{\,3}\frac{\partial \bar{p}_0}{\partial \theta}\right) + \left(\frac{D}{L}\right)^2 \frac{\partial}{\partial \bar{z}}\left(\bar{h}_0^{\,3}\frac{\partial \bar{p}_0}{\partial \bar{z}}\right) = 6\frac{\partial \bar{h}_0}{\partial \theta} - 2\times R_e^* \times \left[\frac{\partial}{\partial \theta}\left(\bar{h}_0 \times I_X\right) + \left(\frac{D}{L}\right)\frac{\partial}{\partial \bar{z}}\left(\bar{h}_0 \times I_z\right)\right] \quad (13)$$

Where,

$$I_X = \frac{\bar{h}_0}{2}\left[\begin{array}{l} -\frac{1}{3}\left(1 - \frac{1}{2} Q_\theta + \frac{1}{10} Q_\theta^{\,2}\right)\frac{\partial \bar{h}_0}{\partial \theta} + \frac{1}{3}\bar{h}_0 \left(\frac{1}{5} Q_\theta - \frac{1}{2}\right)\frac{\partial Q_\theta}{\partial \theta} + \\ \frac{1}{30}\left(\frac{D}{L}\right)\bar{h}_0\, Q_z \frac{\partial Q_\theta}{\partial \bar{z}} + \frac{1}{6}\left(\frac{D}{L}\right)\bar{h}_0 \left(\frac{1}{5} Q_\theta - \frac{1}{2}\right)\frac{\partial Q_z}{\partial \bar{z}} \end{array}\right] \quad (14)$$

and

$$I_Z = \frac{\bar{h}_0}{2}\left[\begin{array}{l} -\frac{1}{6} Q_z \left(\frac{1}{5} Q_\theta - \frac{1}{2}\right)\frac{\partial \bar{h}_0}{\partial \theta} - \frac{1}{6}\bar{h}_0 \left(\frac{1}{5} Q_\theta - \frac{1}{2}\right)\frac{\partial Q_z}{\partial \theta} + \\ \frac{1}{30}\bar{h}_0 Q_z \frac{\partial Q_\theta}{\partial \theta} + \frac{1}{15}\left(\frac{D}{L}\right)\bar{h}_0\, Q_z \frac{\partial Q_z}{\partial \bar{z}} \end{array}\right] \quad (15)$$

and also,

$$Q_\theta = \frac{\bar{h}_0^{\,2}}{2}\left(\frac{\partial \bar{p}_0}{\partial \theta}\right) + R_e^* \times I_X \quad (16)$$

$$Q_z = \frac{\bar{h}_0^{\,2}}{2}\left(\frac{D}{L}\right)\left(\frac{\partial \bar{p}_0}{\partial \bar{z}}\right) + R_e^* \times I_Z \quad (17)$$

The steady state fluid film thickness can be written as

$$\bar{h}_0 = 1 + \varepsilon_0 \cos\theta \quad (18)$$

When journal and bearing surface is considered smooth ε_0 is steady state eccentricity ratio and p_0 is the steady state oil film pressure.

B. Considering surface roughness effect:

It has been reported by many researcher that the surface roughness patterns significantly influence the steady state and dynamic characterises of hydrodynamic bearings. Consider two real surfaces with normal film gap h in the sliding motion. Local film thickness h_T is defined to be of the form

$$h_T = h + \delta_1 + \delta_2 \quad (19)$$

Where h is the nominal film thickness (compliance) defined as the distance between mean levels of the two surfaces. δ_1 and δ_2 are the random roughness amplitudes of the two surfaces measured from their mean levels.

We assume δ_1 and δ_2 have a Gaussian distribution of heights with zero mean and standard deviations σ_1 and σ_2 respectively.

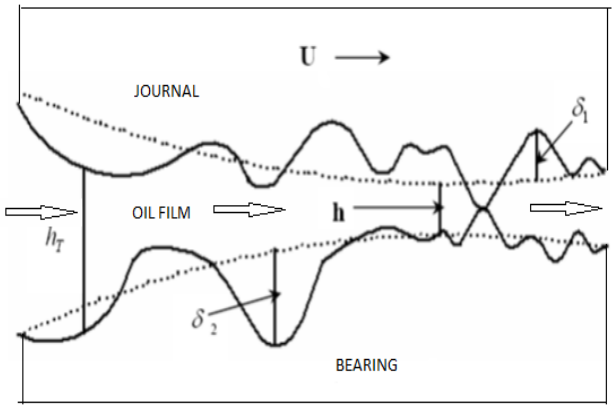

Fig. 2. Two rough surfaces in relative motion

The combined roughness $\delta = \delta_1 + \delta_2$ (20)

and has a variance $\sigma^2 = \sigma_1^{\,2} + \sigma_2^{\,2}$ (21)

The ratio of h/σ is an important parameter showing the effects of surface roughness.

To study surfaces with directional properties the surface characteristic γ can be used. The parameter γ can be viewed as the length to width ratio of a representative asperity. There are mainly three sets of asperity patterns are identified purely

1. Transverse roughness pattern γ <1

2. Isotropic roughness pattern γ =1

3. Longitudinal roughness pattern γ >1

Considering the bearing and journal surface are rough surface having random roughness amplitudes of the two surfaces h_T can be written as

$$h_T = \int_{-h}^{\infty} (h+\delta) f(\delta) d\delta \tag{22}$$

Where $f(\delta)$ is the probability density function of composite roughness. Where δ_1 *and* δ_2 are the random roughness amplitudes of the two surfaces measured from their mean levels. σ_1 *and* σ_2 are the standard deviations.

For a Gaussian distribution, the normal probability function of δ is

$$f(\delta) = \frac{1}{\sigma\sqrt{2\pi}} e^{-\frac{\delta^2}{2\sigma^2}} \tag{23}$$

From equation (22) and (23) we have

$$h_T = \frac{1}{\sigma\sqrt{2\pi}} \int_{-h}^{\infty} (h+\delta) e^{-\frac{\delta^2}{2\sigma^2}} d\delta \tag{24}$$

After integration we have

$$\bar{h}_T = \frac{\bar{h}}{2}\left[1 + erf\left(\frac{\Lambda\,\bar{h}}{\sqrt{2}}\right)\right] + \frac{\bar{\sigma}}{\sqrt{2\pi}} e^{-\bar{h}^2/2\bar{\sigma}^2} \tag{25}$$

Where, $\bar{\sigma}=\frac{\sigma}{c}$, $\bar{h}_T=\frac{h_T}{c}$ and $\Lambda=\frac{c}{\sigma}=\frac{1}{\bar{\sigma}}$.

Where, Λ is called surface roughness parameter.

$$\bar{h}_T=\frac{\bar{h}}{2}\left[1+erf\left(\frac{\Lambda\,\bar{h}}{\sqrt{2}}\right)\right]+\frac{1}{\Lambda\sqrt{2\pi}}\,e^{-0.5*\left(\Lambda\bar{h}\right)^2} \tag{26}$$

Differentiating $\bar{h}_T$ with respect to $x, and\ z$, we get

$$\frac{\partial\bar{h}_T}{\partial\theta}=\frac{1}{2}\left[1+erf\left(\frac{\Lambda\,\bar{h}}{\sqrt{2}}\right)\right]\frac{\partial\bar{h}}{\partial\theta}=\frac{1}{2}\left[1+erf\left(\frac{\Lambda\,\bar{h}}{\sqrt{2}}\right)\right]\times\left(-\varepsilon\sin\theta\right) \tag{27}$$

$$\frac{\partial\bar{h}_T}{\partial\bar{z}}=\frac{1}{2}\left[1+erf\left(\frac{\Lambda\,\bar{h}}{\sqrt{2}}\right)\right]\frac{\partial\bar{h}}{\partial\bar{z}}=0 \tag{28}$$

As $\frac{\partial\bar{h}}{\partial\bar{z}}=0$

C. Pressure Flow Factors:

Patir and Cheng [1] and [2] introduced pressure flow factors ϕ_x and ϕ_z in circumferential and axial direction are obtained through numerical simulation. The pressure flow simulation factors are given by the empirical relation of the form:

$$\phi_x=1-Ce^{-rH}\quad for\ \gamma\le 1 \tag{29}$$

$$\phi_x=1+CH^{-r}\quad for\ \gamma>1 \tag{30}$$

Where $H=\frac{h}{\sigma}$. The constants C and r are given as a

functions of γ in Table. 1

ϕ_z is equal to ϕ_x value corresponding to the directional properties of the z profile. In functional form it is given as:

$$\phi_z\left(\frac{h}{\sigma},\gamma\right)=\phi_x\left(\frac{h}{\sigma},\frac{1}{\gamma}\right) \tag{31}$$

TABLE 1. COEFFICIENTS OF EQUATIONS (29), (30) FOR ϕ_x

γ	C	r	Range
1/9	1. 48	0. 42	H > 1
1/6	1. 38	0. 42	H > 1
1/3	1. 18	0. 42	H > 0. 75
1	0. 90	0. 56	H > 0. 5
3	0. 225	1. 5	H > 0. 5
6	0. 520	1. 5	H > 0. 5
9	0. 870	1. 5	H > 0. 5

D. Shear Flow Factors:

Similar to the pressure flow factors, the shear flow factor is a function of the film thickness and roughness parameters only. However, unlike ϕ_x which only depends on the statistics of the combined roughness δ, and the shear flow factors depends on the statistical parameter of $\delta_1 \text{ and } \delta_2$ separately . Therefore, ϕ_s is a function of h/σ, the standard deviations $\sigma_1 \text{ and } \sigma_2$ and the surface pattern parameters γ_1 and γ_2 of the two opposing surfaces. Through numerical experimentation, ϕ_s is found to depend on these parameters through the functional form:

$$\phi_s = V_{r1}\Phi_s\left(\frac{h}{\sigma},\gamma_1\right) - V_{r2}\Phi_s\left(\frac{h}{\sigma},\gamma_2\right) \tag{32}$$

Where V_{r1} and V_{r2} are the variance ratios given by:

$$V_{r1} = \left(\frac{\sigma_1}{\sigma}\right)^2 , \; V_{r2} = \left(\frac{\sigma_2}{\sigma}\right)^2 = 1 - V_{r1} \tag{33}$$

Φ_s is a positive function of h/σ and the surface pattern parameter of the given surface.

The shear flow factor Φ_s is plotted as a function of h/σ and γ in [1, 2]. starting with zero for purely longitudinal roughness $(\gamma=\infty)$, the shear flow factor increases with decreasing γ, and retains highest value for purely transverse roughness $(\gamma=0)$. Through numerical simulation and using nonlinear least square program they are of the form:

$$\Phi_s = A_1 H^{\alpha_1} e^{-\alpha_2 H + \alpha_3 H^2} \quad H \le 5 \tag{34}$$

Where $H = \frac{h}{\sigma}$, For extrapolationbeyond $H = 5$ the following relation should be used:

$$\Phi_s = A_2 e^{-0.25H} \quad H > 5 \tag{35}$$

The coefficients $A_1, A_2, \alpha_1, \alpha_2, \alpha_3$ are listed as functions of γ in Table 2.

TABLE 2: COEFFICIENTS OF EQUATIONS (32), (33) FOR Φ_s (RANGE $H > 0.5$)

γ	A_1	α_1	α_2	α_3	A_2
1/9	2. 046	1. 12	0. 78	0. 03	1. 856
1/6	1. 962	1. 08	0. 77	0. 03	1. 754
1/3	1. 858	1. 01	0. 76	0. 03	1. 561
1	1. 899	0. 98	0. 92	0. 05	1. 126
3	1. 560	0. 85	1. 13	0. 08	0. 556
6	1. 290	0. 62	1. 09	0. 08	0. 388
9	1. 011	0. 54	1. 07	0. 08	0. 295

Now introducing pressure flow factors $\phi_x \text{ and } \phi_z$ with shear flow factors ϕ_s we get modified Reynolds's equations considering combined effect of fluid inertia and surface roughness in dimensionless form under steady state condition as:

$$\frac{\partial}{\partial\theta}\left(\phi_X \bar{h}_0^{\,3}\frac{\partial \bar{p}_0}{\partial\theta}\right) + \left(\frac{D}{L}\right)^2 \frac{\partial}{\partial \bar{z}}\left(\phi_z \bar{h}_0^{\,3}\frac{\partial \bar{p}_0}{\partial \bar{z}}\right) = 6\frac{\partial \bar{h}_{T_0}}{\partial\theta} + 6\bar{\sigma}\frac{\partial\phi_s}{\partial\theta} - 2\times R_e^* \times\left[\frac{\partial}{\partial\theta}\left(\bar{h}_{T_0}\times I_X\right) + \left(\frac{D}{L}\right)\frac{\partial}{\partial \bar{z}}\left(\bar{h}_{T_0}\times I_z\right)\right] \tag{36}$$

Or,

$$\frac{\partial}{\partial\theta}\left(\phi_X\,\bar{h}_0^{\,3}\frac{\partial\bar{p}_0}{\partial\theta}\right)+\left(\frac{D}{L}\right)^2\frac{\partial}{\partial\bar{z}}\left(\phi_z\,\bar{h}_0^{\,3}\frac{\partial\bar{p}_0}{\partial\bar{z}}\right)=3\times\left[1+erf\left(\frac{\Lambda\,\bar{h}_0}{\sqrt{2}}\right)\right]\times\left(-\varepsilon\sin\theta\right)+$$

$$6\,\bar{\sigma}\frac{\partial\phi_S}{\partial\theta}-2\times R_e^{*}\times\left[\frac{\partial}{\partial\theta}\left(\bar{h}_{T_0}\times I_X\right)+\left(\frac{D}{L}\right)\frac{\partial}{\partial\bar{z}}\left(\bar{h}_{T_0}\times I_z\right)\right] \qquad (37)$$

Where, I_x and I_z are same as equation (14) and (15) above,

Boundary conditions for equation (37) are as follows

1. The pressure at the ends of the bearing is assumed to be zero (ambient): $\bar{p}_0\ (\theta,\ \pm1)=0$

2. The pressure distribution is symmetrical about the mid-plane of the bearing: $\frac{\partial\bar{p}_0}{\partial\bar{z}}\ (\theta,\ 0)=0$

3. Cavitation boundary condition is given by:

$$\frac{\partial\bar{p}_0}{\partial\theta}\left(\theta_2,\ \bar{z}\right)=0\ \ and\ \ \bar{p}_0\left(\theta,\bar{z}\right)=0\ \ for\ \theta_1\geq\theta\geq\theta_2$$

The equations (14), (15), (16), (17) and (37) are first expressed in finite difference form and solved simultaneously using Gauss-Siedel method in a finite difference scheme.

III. METHOD OF SOLUTION

To find out steady-state pressure all the equations (14), (15), (16), (17), (18) and (37) are expressed in finite difference form along with the boundary conditions. First for $(\varepsilon_0\leq0.2)$ the pressure distribution and flow parameters Q_θ and Q_z are evaluated from inertia less $(\mathrm{Re}^{*}=0)$solution, i. e., solving classical Reynold's equation. These values are then used as initial value of flow parameters to solve Equations (16) and (17) simultaneously for Q_θ and Q_z Using Gauss-Siedel method in a finite difference scheme. Then update I_x & I_z and calculate Q_θ and Q_z for use to solve Equation (37) with particular surface roughness pattern $(\gamma)$and surface roughness parameter $(\Lambda)$for new pressure p distribution with inertia effect by using a successive over relaxation scheme. The latest values of Q_θ, Q_z and p are used simultaneously with appropriate iteration scheme to solve the set of equations until all variables converges. The convergence criterion adopted for pressure is $\left|\left(1-\left(\sum\bar{p}_{new}\Big/\sum\bar{p}_{old}\right)\right)\leq10^{-5}\right|$ and also same criterion for Q_θ and Q_z. For higher eccentricity ratios $(\varepsilon_0>0.2)$the initial values for the variables are taken from the results corresponding to the previous eccentricity ratios. Very small increment in ε is to be provided as Re^{*} increases. The procedure converges up to a value of Re^{*}=1.5 which should be good enough for the present study. Since the bearing is symmetrical about its central plane ($\bar{z}$ =0), only one half of the bearing needs to be considered for the analysis.

A. *Fluid film forces:*

The non-dimensional fluid film forces along line of centers and perpendicular to the line of centers are given by

$$\bar{F}_{r_0}\left(=\frac{F_{r_0}\,c^2}{\eta\omega R^3L}\right)=\int_0^1\int_{\theta_1}^{\theta_2}\bar{p}_0\cos\theta\,d\theta\,d\,\bar{z} \qquad (38)$$

$$\bar{F}_{\phi_0}\left(=\frac{F_{\phi_0}\,c^2}{\eta\omega R^3L}\right)=\int_0^1\int_{\theta_1}^{\theta_2}\bar{p}_0\sin d\theta\,d\,\bar{z} \qquad (39)$$

where θ_1 and θ_2 are angular coordinates at which the fluid film commences and cavitates respectively.

B. *Steady state load:*

The steady state non-dimensional load and attitude angle are given by

$$\bar{W}_0 = \sqrt{\left(\bar{F}_{r_0}{}^2 + \bar{F}_{\phi_0}{}^2\right)} \tag{40}$$

$$\phi_o = \tan^{-1}\left(\frac{-\bar{F}_{\phi_0}}{\bar{F}_{r_0}}\right) \tag{41}$$

Since the steady state film pressure distribution has been obtained at all the mesh points, integration of equations (38) and (39) can be easily performed numerically by using Simpson's 1/ 3 rd. rule to get $\bar{F}_r$ and $\bar{F}_\phi$. The steady state load $\bar{W}_0$ and the attitude angle (ϕ_0) are calculated using equations (40) and (41).

C. *End Flow:*

End flow from the bearing consists of two parts: (a) from the clearance space (b) from the open ends of the bush, But flow from the open ends of the bush is usually very small compared with that from the clearance space, and hence only flow through clearance space is calculated .
Flow from the clearance space is given by

$$Q = 2\int_0^{h_0}\int_0^{2\pi} (w)_{z=\frac{L}{2}}\, R\, d\theta\, d\, y \tag{42}$$

Substituting the value of w from the relation (8) andequation (17) applying appropriate boundary conditions into equation (42) and performing integration with respect to y and non-dimensionalising, the equation will assume the form

$$\bar{Q} = -\frac{1}{6}\int_0^{2\pi}\left\{\frac{1}{2}\bar{h}_{T_0}{}^3\left(\frac{D}{L}\right)\left(\frac{\partial \bar{p}_0}{\partial \bar{z}}\right)_{\bar{z}=1} + \bar{h}_{T_0}\,\mathrm{Re}^*\left(I_z\right)_{z=1}.\right\} d\theta \tag{43}$$

where, $\bar{Q} = \dfrac{Q}{\omega R^2 c}$

Non-dimensional end flow can thus be calculated first by finding numerically $\left(\dfrac{\partial \bar{p}_0}{\partial \bar{z}}\right)_{\bar{z}=1}$ and then numerical integration, once, the pressure distribution in the film region is known.

The present steady state results (considering only fluid inertia effect) are compared to the results of Kakoty et. al., [7] and Chen & Chen [13] (for L/D=1.0) as given in Table 3. These three results are in good agreement.

The theoretical study has been done considering only Inertia effects and also considering surface roughness effect separately before doing the same for combined effects. The results have been compared with available data of researchers.

TABLE 3: COMPARISON OF STEADY-STATE CHARACTERISTICS OF OIL JOURNAL BEARINGS FOR L/D=1.0 WITH FLUID INERTIA EFFECT ONLY

Re*	ε_0	$\bar{W}_0$	$\bar{W}_0$	$\bar{W}_0$	ϕ_0	ϕ_0	ϕ_0
		Present	Kakoty	Chen-Chen	Present	Kakoty	Chen-Chen
0	0. 2	0. 503	0. 5042	0. 501	77. 541	73. 71	73. 90
	0. 5	1. 759	1. 7903	1. 779	58. 398	56. 64	56. 80
	0. 8	7. 085	7. 4597	7. 146	36. 345	34. 66	36. 20
	0. 9	16. 89	17. 713	16. 98	26. 175	23. 90	26. 40
0. 28	0. 2	0. 504	0. 5055	0. 504	77. 927	73. 75	74. 20
	0. 5	1. 794	1. 7980	1. 785	57. 725	56. 72	57. 00
	0. 8	7. 194	7. 4837	7. 151	36. 310	34. 72	36. 30

	0. 9	17. 04	17. 761	16. 99	26. 240	23. 93	26. 40
0. 56	0. 2	0. 505	0. 5070	0. 505	78. 311	73. 79	74. 50
	0. 5	1. 829	1. 8058	1. 790	57. 114	56. 79	57. 20
	0. 8	7. 301	7. 5081	7. 159	36. 291	34. 78	36. 40
	0. 9	17. 19	17. 809	17. 00	26. 308	23. 97	26. 40
1. 4	0. 2	0. 509	0. 5112	0. 508	79. 449	73. 95	75. 30
	0. 5	1. 934	1. 8307	1. 587	55. 459	57. 05	58. 00
	0. 8	7. 609	7. 5852	7. 1870	36. 2559	35. 02	36. 70
	0. 9	17. 62	------	17. 03	26. 509	----	26. 60

TABLE 4 . COMPARISON OF STEADY- STATE LOAD CAPACITY, ATTITUDE ANGLE, SIDE LEAKAGE WITH AVAILABLE RESULT OF HAMROCK AND B. C. MAJUMDAR[10] AND PINKUS AND STERNLICHT [4] FOR THE FOLLOWING BEARING PARAMETERS CONSIDERING SURFACE ROUGHNESS EFFECT ONLY [$L/D=1.0$, $\Lambda=6.0$, $V_{r1}=0.5$, $\gamma=1.0$]

ε_0	$\bar{W}_0$			ϕ_0			Q_0		
	(a)	(b)	(c)	(a)	(b)	(c)	(a)	(b)	(c)
0. 2	0. 08	0. 08	0. 08	76. 8	73. 6	74. 0	0. 31	0. 31	0. 32
0. 4	0. 19	0. 19	0. 20	63. 5	61. 6	62. 0	0. 61	0. 61	0. 61
0. 5	0. 42	0. 45	0. 44	49. 5	48. 6	50. 0	0. 89	0. 93	0. 94
0. 8	1. 42	1. 46	1. 18	33. 5	33. 3	36. 0	1. 09	1. 29	1. 24

(a)-Present

(b)-Hamrock and B. C. Majumdar[10]

(c)-Pinkus and Sternlicht[4]

TABLE 5. VARIATION OF STEADY-STATE LOAD AND SIDE LEAKAGE WITH VARIOUS LENGTH-TO-DAIMETER RATIOS CONSIDERING SURFACE ROUGHNESS EFFECT ONLY $\varepsilon_0=0.2$, $V_{r1}=0.5$

L/D	γ	Λ	$\bar{W}_0$ (a)	$\bar{W}_0$ (b)	$\bar{Q}$ (a)	$\bar{Q}$ (b)
1	1/6	1	0. 056	0. 054	0. 290	0. 320
		2	0. 074	0. 074	0. 324	0. 350
		3	0. 077	0. 075	0. 322	0. 330
		4	0. 076	0. 075	0. 317	0. 320
	1	1	0. 118	0. 131	0. 260	0. 280
		2	0. 097	0. 105	0. 302	0. 300
		3	0. 086	0. 091	0. 308	0. 310
		4	0. 080	0. 084	0. 308	0. 310
	6	1	0. 157	0. 157	0. 154	0. 090
		2	0. 115	0. 127	0. 262	0. 220
		3	0. 096	0. 105	0. 288	0. 270
		4	0. 086	0. 097	0. 297	0. 280
	1/6	1	0. 014	0. 013	0. 146	0. 080
		2	0. 020	0. 020	0. 168	0. 090

0. 5		3	0. 021	0. 022	0. 171	0. 090
		4	0. 022	0. 022	0. 170	0. 090
	1	1	0. 075	0. 104	0. 142	0. 070
		2	0. 040	0. 050	0. 165	0. 090
		3	0. 031	0. 036	0. 168	0. 090
		4	0. 027	0. 030	0. 169	0. 090
	6	1	0. 075	0. 104	0. 114	0. 040
		2	0. 040	0. 050	0. 157	0. 080
		3	0. 031	0. 036	0. 165	0. 080
		4	0. 027	0. 030	0. 167	0. 090
2. 0	1/6	1	0. 215	0. 203	0. 565	1. 280
		2	0. 236	0. 209	0. 571	1. 080
		3	0. 223	0. 209	0. 541	1. 010
		4	0. 212	0. 196	0. 518	0. 940
	1	1	0. 311	0. 309	0. 409	0. 690
		2	0. 255	0. 247	0. 473	0. 800
		3	0. 224	0. 215	0. 482	0. 820
		4	0. 209	0. 197	0. 481	0. 820
	6	1	0. 235	0. 210	0. 171	0. 120
		2	0. 239	0. 211	0. 353	0. 490
		3	0. 220	0. 202	0. 416	0. 640
		4	0. 208	0. 192	0. 442	0. 710

(a) . . . . . Present

(b) . . . . . Hamrock-B. C. Majumdar [10]

A. Effect of modified Reynold'snumber **(** Re^{*} ***) on load carrying capacity:***

The present steady state results with respect to load carrying capacity and attitude angle with fluid inertia effect only are compared to the results of Kakoty et. al., [7] and Chen & Chen [13] (for $L/D=1.0$) as given in Table 3.

These three results are in good agreement. A slight decrease in load capacity with modified Reynolds number (Re^{*}) is observed in the present study compare to others. In the present study it is observed attitude angle increases slightly for all eccentricity ratios compare to others.

B. Comparison of Steady state Load Capacity, Attitude angle, Side Leakage:

The present steady state results with respect to load carrying capacity and attitude angle with surface roughness effect arecompared to the result of Hamrock and B. C. Majumdar [10] and Pinkus and Sternlicht [4] for roughness effect only as shown in Table 4. These results are in good agreement.

C. ***Effect of Steady-State load and side leakage with various Length-to-Daimeter ratios:***

The present steady state results with respect to load carrying capacity and side leakage with surface roughness effect are compared to the results of Hamrock and B. C. Majumdar[10] for roughness effect only as shown in Table 5. For $L/D=1.0$ and various Λ and γ the results are in good agreement with Hamrock and B. C. Majumdar [10] and for higher and lower value of L/D the load carrying capacity values are quite matching with the value of Hamrock and B. C. Majumdar [10] but side leakage values are not matching.

IV. RESULTS AND DISCUSSIONS

A. *Effect of Modified Reynold's Number (Re*) with eccentricity ratio considering inertia effect only*:

Figure 3.Variation of steady-state load with ecentricity ratio for fluid film inertia effect and different modified Reynolds number

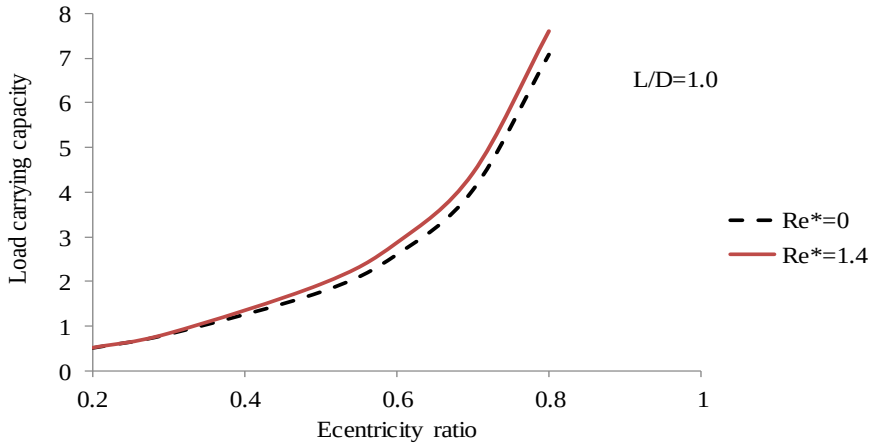

Figure 3 shows the load carrying capacity of journal bearings as a function of eccentricity ratio (ε_0) with fluid film inertia effect when $L/D=1.0$. A study of the figure reveals that as eccentricity ratio increases the dimensionless load increases when other parameters remain constant. It is also observed that the load parameter increases with the increase in modified Reynold's number which means fluid inertia increases load carrying capacity. For the higher eccentricity ratio $\varepsilon_0 > 0.7$ the load parameters increases sharply.

B. *Effect of variance ratio with surface roughness parameter for surface roughness effect only*:

Figure 4. Variation of steady-state load carrying capacity with roughness parameter for different variance ratio.

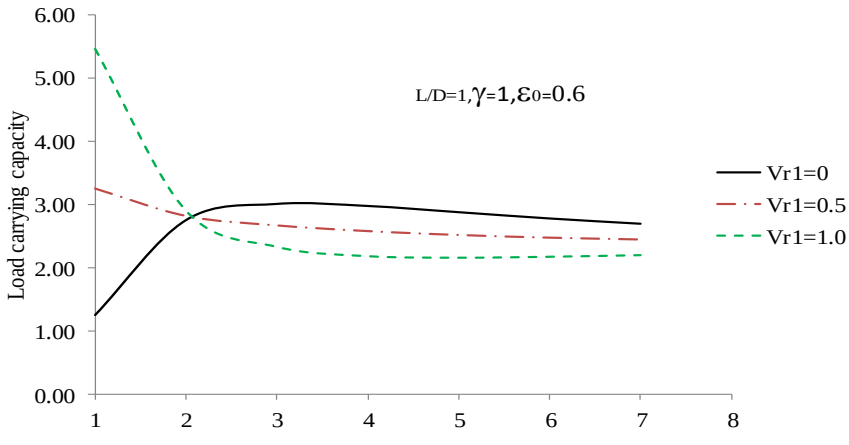

Figure 4 shows steady state dimensionless load capacity of journal bearing as a function of surface roughness parameter Λ with different variance ratio. It is observed from the figure the load carrying capacity is increases when $\Lambda < 3.0$ and variance ratio $V_{r1} = 1.0$ and when $\Lambda > 3.0$ the variation is almost constant. For variance ratio ($V_{r1} = 0.0$) it decreases when $\Lambda < 3.0$ and thereafter when $\Lambda > 3.0$ the variation is almost constant. Load carrying capacity almost constant when $\Lambda > 3.0$ for variance ratio ($V_{r1} = 0.5$) the curve lies in between other variance ratio.

C. Effect of Modified Reynold's Number (Re*) with eccentricity ratio considering inertia and surface roughness effect:

Figure 5.Variation of side leakage with ecentricity ratio for fluid film inertia and surface roughness effect.

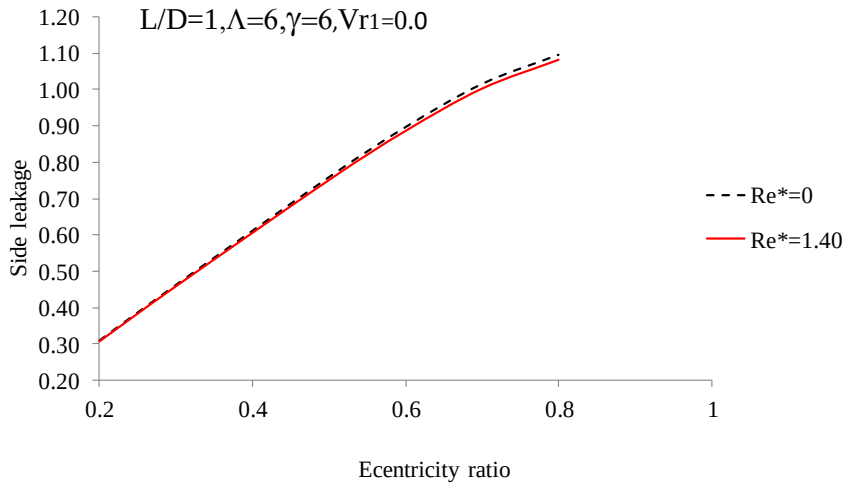

Figure 5 shows steady state side leakage of journal bearing as a function of eccentricity ratio (ε_0) with both fluid inertia and surface roughness effect for L/D=1.0 with modified Reynolds number as a parameter. It is observed from the figure the dimensionless side leakage increases with eccentricity ratio (ε_0). The side leakage is slightly decreases when both effects has been considered. But the effect of fluid film inertia is insignificant.

D. Effect of Modified Reynold's Number (Re*) with eccentricity ratio considering inertia and surface roughness effect:

Figure 6.Variation of steady-state load with ecentricity ratio for fluid film inertia and surface roughness effect.

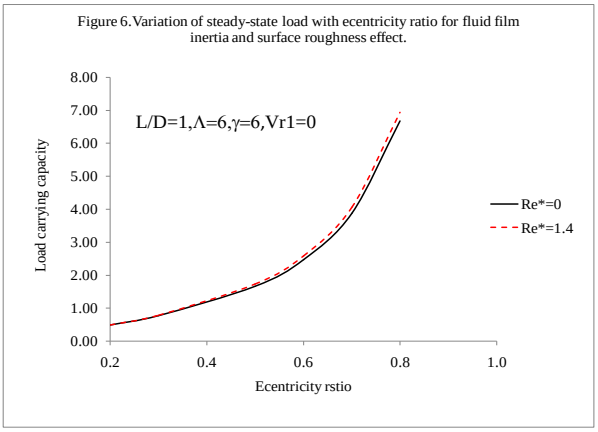

Figure 6 shows steady state load carrying capacity of journal bearing as a function of eccentricity ratio (ε_0) with fluid film inertia and surface roughness effect for L/D=1.0 with modified Reynolds number as a parameter. It is observed from the figure that the dimensionless load increases with increase in eccentricity ratio (ε_0) and fluid inertia improves the load carrying capacity.

E. Effect of eccentricity ratio with attitude angle considering inertia and surface roughness effect:

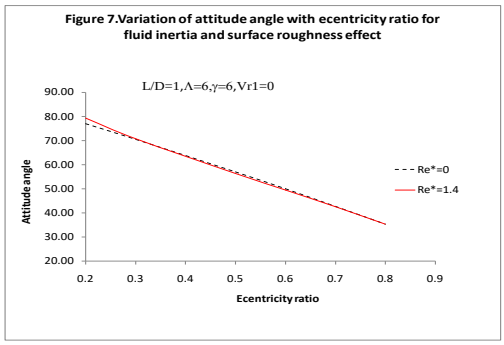

Figure 7 shows the variation of attitude angle with eccentricity ratio for different modified Reynolds number when combine fluid inertia and surface roughness effect are considered. . It is observed attitude angle decreases as eccentricity ratio increases almost linearly. The variation is insignificant with respect to modified Reynolds number.

F. Effect of smooth surfaces, surface roughness, fluid inertia and combined inertia and roughness on eccentricity ratio:

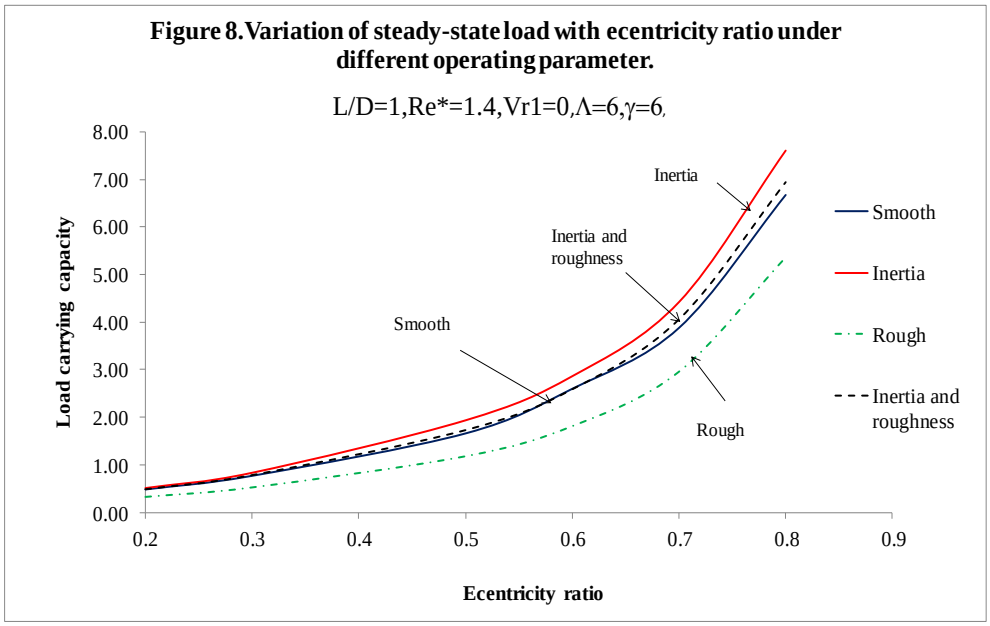

Figure 8 shows steady state load carrying capacity of journal bearing as a function eccentricity ratio (ε_0) considering four different condition as with the effect of fluid film inertia, smooth surface, rough surface and combined effect of fluid film inertia and rough surface for L/D=1.0. It is observed from the figure that steady state load capacity is maximum when fluid film inertia effect only considered and minimum when we consider rough surface effect only. Also we observed at $(\varepsilon_0 > 0.5)$the load carrying capacity is increased marginally for combine effect in comparison to smooth surface.

G. Effect of Roughness Parameter over Roughness Pattern and Inertia effect:

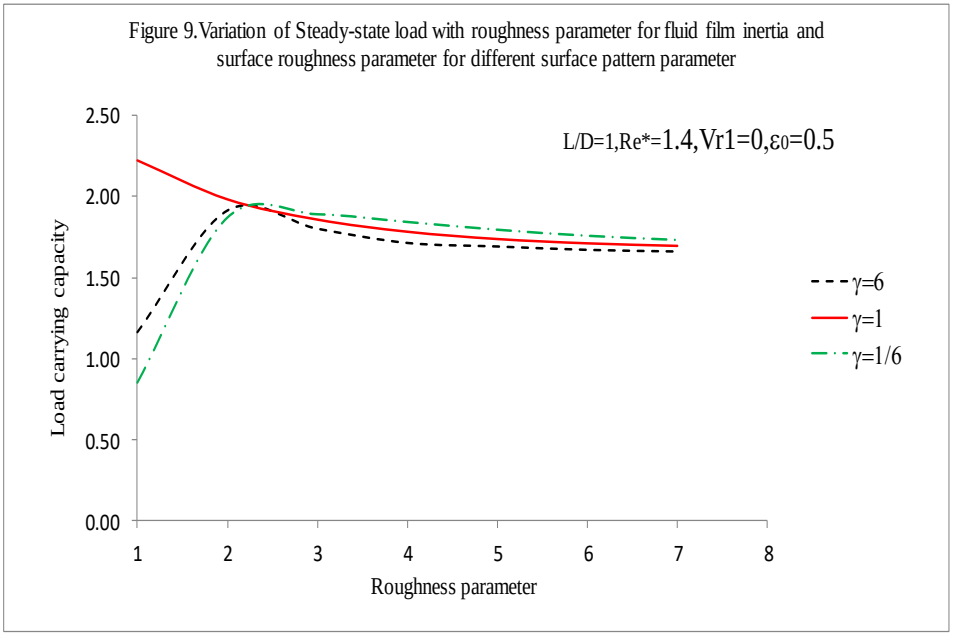

Figure 9. shows variation of steady state load with roughness parameter considering combined effect of fluid film inertia and surface roughness for different surface pattern parameter. It is observed that steady state load is maximum for roughness pattern parameter ($\gamma = 1.0$) and minimum for ($\gamma = 1/6$) for roughness parameter ($\Lambda < 3.0$) and for roughness pattern parameter ($\Lambda > 3.0$) it observed the variation is almost constant.

H. Effect of Roughness Parameter over Roughness Pattern and Inertia effect:

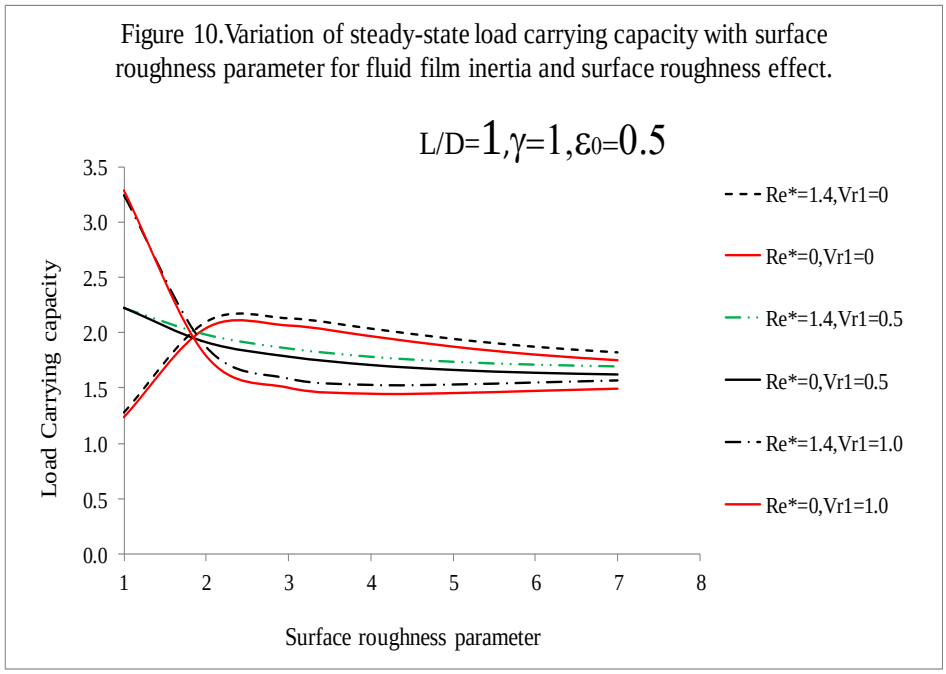

Figure. 10 shows steady state dimensionless load capacity of journal bearing with fluid film inertia and surface roughness effect as a function of roughness parameter Λ for different variance ratio and modified Reynolds number (Re^*) combination and for L/D=1.0 . It is observed from the figure dimensionless load capacity is maximum for $V_{r1} = 1.0$, Re*=0.0 and minimum for $V_{r1} = 0.0$, Re*=0.0.

V. CONCLUSIONS

1. It is important to note that the load carrying capacity increases with increase in modified Reynold's number and eccentricity ratio.
2. When the roughness parameter $\Lambda \geq 6.0$ the results obtained from the present method of solution considering combine effect are reasonably in similar nature compared with surface roughness effect only and nature of curve are similar with available solution.
3. The steady-state load carrying capacity increases when surface roughness parameter ($\Lambda < 3.0$) and journal surface is rough (i. e $V_{r1} = 1.0$).
4. The steady-state load carrying capacity increases marginally when surface roughness parameter ($\Lambda < 3.0$) and both the journal and bearing are of same roughness structure (i. e $V_{r1} = 0.5$).
5. The steady-state load carrying capacity decreases when surface roughness parameter ($\Lambda < 3.0$) and journal surface is smooth (i. e $V_{r1} = 0.0$).
6. It is observed that when both surfaces have the same roughness structure then with isotropic oriented surface pattern $\gamma = 1.0$ gives maximum steady state load carrying capacity and transversely oriented surface pattern $\gamma = 1/6$ gives the minimum steady state load carrying capacity for eccentricity ratio $(\varepsilon_0 < 0.2)$.
7. Side leakage increases with increase in eccentricity ratio for inertia and surface roughness effect.
8. Attitude angle decreases linearly with eccentricity ratio for inertia and surface roughness effect.

VI. NOMENCLATURE

c Radial clearance (m)
D Diameter of Journal (m)
e eccentricity (m)
F_{r_0}, F_{ϕ_0} Steady state hydrodynamic film forces (N).
$\bar{F}_{r_0}, \bar{F}_{\phi_0}$ Dimensionless steady state hydrodynamic film forces
h_0 Steady state nominal Film thickness, (m)
$\bar{h}_0$ Dimensionless Steady state nominal Film thickness
L Length of the bearing in m
p Film pressure in Pa
$\bar{p}$ dimensionless film pressure $\left(\frac{pc^2}{\eta\omega R^2}\right)$
R radius of journal in m
R_e Reynolds number, $\frac{\rho c R\omega}{\eta}$
R^*_e Modified Reynolds number, $\left(\frac{c}{R}\right)R_e$
u, v, w Velocity components in x, y, z directions inm/s
$\bar{u}, \bar{v}, \bar{w}$ Dimensionless velocity components
W_0 Steady-state load bearing capacity in N
$\bar{W}_0$ Dimensionless steady-state load $\frac{W_0 c^2}{\eta\omega R^3 L}$
x, y, z Coordinates
$\theta, \bar{Y}, \bar{Z}$ Dimensionless coordinates, $\frac{x}{R}, \frac{y}{c}, \frac{z}{L/2}$
ε_0 Steady-state eccentricity ratio
ρ Density of the lubricant (kg m^{-3})
ω Angular velocity of journal(rad s^{-1})
ω_p Angular velocity of whirl (rad s^{-1})
η_0 Absolute viscosity of lubricating Film at inlet condition (N s m^{-1})
ϕ Attitude angle
Q_θ Dimensionless flow parameter in θ direction
Q_z Dimensionless flow parameter in $\bar{z}$ direction
$\bar{Q}$ Dimensionless side leakage
θ_1, θ_2 Angular coordinates at which film commences and cavitates.
γ Surface pattern parameter
Λ Roughness Parameter, $\Lambda = c/\sigma$

H h/σ

ϕ_x , ϕ_z Pressure flow factors

Φ_s Shear flow factor

σ Composite r. m. s roughness, $\sigma = \sqrt{\sigma_1^{\,2} + \sigma_2^{\,2}}$

Vr_1 Variance ratio,

REFERENCES

[1] Patir, N. and Cheng, H. S. , 1978, ‘‘An Average Flow Model for Determining Effects of Three-Dimensional Roughness on Partial Hydrodynamic Lubrication, ’’ ASME J. Lubr. Technol. , 100, pp. 12–17.

[2] Patir, N. , and Cheng, H. S. , 1979, ‘‘Application of Average Flow Model to Lubrication Between Rough Sliding Surfaces, ’’ ASME J. Lubrication Technol. , 101, pp. 220–230.

[3] V. N. Constantinescu and S. Galetuse “On the Possibilities of Improving the Accuracy of the Evaluation of Inertia Forces in Laminar and Turbulent Films” *J. Tribol.* Vol 96 (1), 69-77 (Jan 01, 1974) (9 pages), ASME, Journal of Tribology | Volume 96 | Issue 1 |

[4] Pinkus, O. and Sternlicht, B. , *Theory of Hydrodynamic Lubrication*, New York, McGraw-Hill (1961).

[5] Banerjee Mihir B. , Shandil R. G. , and Katyal S. P. ”A Nonlinear Theory of Hydrodynamic Lubrication” Journal of Mathematical Analysis and Applications 117, 48-56(1986)

[6] Tichy, J. , and Bou-Said, B. , 1991, “Hydrodynamic Lubrication and Bearing Behaviour With Impulsive Loads, ” STLE Tribol. Trans. , 34, pp. 505–512.

[7] Kakoty S. K. and Majumdar B. C. , “Effect of Fluid Inertia on Stability of Oil Journal Bearing”. ASME Journal of Tribology, Vol 122, pp 741-745, October 2000

[8] Elrod, H. G. , 1979, ‘‘A General Theory for Laminar Lubrication With Reynolds Roughness, ’’ ASME J. Lubr. Technol. , 101, pp. 8–14.

[9] Tripp, J. H. , 1983, ‘‘Surface Roughness Effects in Hydrodynamic Lubrication: The Flow Factor Method, ’’ ASME J. Lubr. Technol. , 105, pp. 458–464.

[10] B. C. Majumdar and B. J Hamrock, Surface Roughness Effect on Finite Oil Journal Bearing NASA Technical Memorandum 82639

[11] Tonder. K. , 1980, ”Simulation of the Lubrication of Isotropically Rough surfaces, ”ASLE Trans. , vol 23, No. 3, July, pp. 326-333

[12] Greenwood, J. A. , and Tripp, J. H. , ”The contact of Two Nominally Flat Rough surfaces. ”Proc. Inst. Mech. Eng (London)”, vol. 185, 1970-71, pp. 625-633

[13] Tripp, J. H. , 1983, ‘‘Surface Roughness Effects in Hydrodynamic Lubrication: The Flow Factor Method, ’’ ASME J. Lubr. Technol. , 105, pp. 458–464

[14] Chen, C. H. and Chen, C. K. , “The influence of fluid inertia on the operating characteristics of finite journal bearings”, Wear, Vol. 131, (1989), pp. 229-240

[15] E. Sujith Prasad, T. Nagaraju& J. PremSagar“ Thermohydrodynamic performance of a journal bearing with 3d-surface roughness and fluid inertia effects” International Journal of Applied Research in Mechanical Engineering (IJARME) ISSN: 2231 –5950, Volume-2, Issue-1, 2012.